

Supplementary Material: Towards a MEMS-based Adaptive LIDAR

Francesco Pittaluga*
NEC Labs America
francescopittaluga@nec-labs.com

Zaid Tasneem*
University of Florida
ztasneem@ufl.edu

Justin Folden*
University of Florida
jfolden@ufl.edu

Brevin Tilmon
University of Florida
btilmon@ufl.edu

Ayan Chakrabarti
Washington University in St. Louis
ayan@wustl.edu

Sanjeev J. Koppal
University of Florida
sjkoppal@ece.ufl.edu

A. Derivations

Here we derive all the formulae in Table 1 for the three designs. We have provided the ray diagrams of the designs in Fig. A1 and we have reproduced Table A1 here.

A.1. Volume

For the retroreflection and single detector, the volume of the camera is a cone whose vertex is the location of the single detector. From the ray diagrams and from the equation of the volume of a cone, this is easily seen to be $\frac{\pi u w^2}{12}$ for the retroreflector and $\frac{\pi u A^2}{12}$ for the single detector. For the receiver array the volume is the entire enclosure, given by the volume of a cuboid, $u * A * A$.

A.2. FOV

The retroreceiver has the exact same FOV as the mirror, by definition. From A1(b), the FOV of the receiver array is given by the vertex angle of the cone at the central pixel, given by $2\text{atan}(\frac{A}{2u})$, bounded by the FOV of the mirror. This assumes the receiver and transmitter are close enough to ignore angular overlap issues.

To find the FOV of the single detector, consider the diagram in Fig. A3, where the single detector is focused on the laser dot at distance Z from the sensor. From similar triangles, the kernel size is given by first finding the in-focus plane at u' from the lens equation

$$\frac{1}{f} = \frac{1}{u'} + \frac{1}{Z} \quad (\text{A1})$$

and so $u' = \frac{fZ}{(Z-f)}$. From the two vertex shared similar triangles on the left of the lens, we now have an expression for the kernel size

$$\text{kernel size} = \text{abs}(u - u') * \frac{A}{u'} \quad (\text{A2})$$

Substituting the value of u' , we get an expression for

$$\text{kernel size} = \text{abs}(u - \frac{fZ}{(Z-f)}) * \frac{A}{\frac{fZ}{(Z-f)}} \quad (\text{A3})$$

$$= \frac{A(Z-f)\|(Zu - fu - fZ)\|}{fZ\|Z-f\|} \quad (\text{A4})$$

$$= \frac{A(Z-f)\|\frac{Zu-fu-fZ}{Z-f}\|}{fZ}. \quad (\text{A5})$$

From the figure, the FOV, given by kernelangle is

$$2\text{atan}(\frac{\text{kernel size}}{2u}) = 2\text{atan}(\frac{A(Z-f)\|\frac{Zu-fu-fZ}{Z-f}\|}{2ufZ}) \quad (\text{A6})$$

A.3. Received Radiance (RR)

From Fig. A2, the power from the laser decreases with distance. This is just fall-off from the source, and we represent it here as the area of the laser dot on a fronto-parallel plane. From the figure, this can be calculated from simple trigonometry as

$$2Z\tan(\frac{\omega_{\text{laser}}}{2}), \quad (\text{A7})$$

and we use the reciprocal for the RR as

$$\frac{1}{2Z\tan(\frac{\omega_{\text{laser}}}{2})}. \quad (\text{A8})$$

1. Receiver array: The receiver array is assumed to capture all the available radiance from the laser dot, and so the RR is exactly the same as the power fall-off described above as

*Equal Contribution

Sensor	Technology	Outdoors	Textureless	Adaptive
ELP-960P2CAM	Conventional Passive Stereo	✓	×	×
Kinect v2	Time-of-Flight (LED)	×	✓	×
Intel RealSense	Structured Light Stereo (LED)	✓	✓	×
Velodyne HDL-32E	Time-of-Flight (Laser)	✓	✓	×
Resonance MEMS / Intel L515	Time-of-Flight (Laser)	✓	✓	×
Robosense RS-LiDAR-M1	Solid State Time-of-Flight (Laser)	✓	✓	×
Programmable Light curtains	Adaptive Structured Light	✓	✓	✓
Our sensor	Adaptive LIDAR	✓	✓	✓

Table A1: **Our Adaptive LIDAR vs. other common modalities.**

$$\frac{1}{2Z \tan\left(\frac{\omega_{laser}}{2}\right)}. \quad (\text{A9})$$

2. Retroreflection: As can be seen in the right of Fig. A2, the ratio of the received angle to the transmitted angle gives the fraction of the received radiance from the laser dot. From Fig. A1(a), the single detector receives parallel light of width w_o . For any particular depth Z therefore, the angle subtended by this width at the sensor decreases and is given by

$$\omega_{receiver} = 2 \operatorname{atan}\left(\frac{w_o}{2Z}\right) \quad (\text{A10})$$

and the fraction of the fall-off received is given by

$$\frac{2 \operatorname{atan}\left(\frac{w_o}{2Z}\right)}{\omega_{laser}}. \quad (\text{A11})$$

Multiplying this with the fall-off above gives

$$\frac{2 \operatorname{atan}\left(\frac{w_o}{2Z}\right)}{\omega_{laser}} * \frac{1}{2Z \tan\left(\frac{\omega_{laser}}{2}\right)} \quad (\text{A12})$$

$$= \frac{\operatorname{atan}\left(\frac{w_o}{2Z}\right)}{\omega_{laser} Z \tan\left(\frac{\omega_{laser}}{2}\right)}. \quad (\text{A13})$$

Note this assumes that $\omega_{receiver} < \omega_{laser}$, and if this is not the case then a max function must be added so that $\omega_{receiver}$ does not exceed ω_{laser} .

3. Single detector: We just reduce the fall-off by the ker-angle calculated before, and therefore the RR is

$$\frac{1}{\kerangle * 2Z \tan\left(\frac{\omega_{laser}}{2}\right)} \quad (\text{A14})$$

$$= \frac{1}{4Z \operatorname{atan}\left(\frac{A(Z-f) \parallel \frac{Zu-fu-fZ}{Z-f} \parallel}{2u f Z}\right) \tan\left(\frac{\omega_{laser}}{2}\right)} \quad (\text{A15})$$

B. Single detector and proposed modification

Our approach is based on a simple observation; placing the image plane between the lens and the focus, i.e. $v < f$, will guarantee that the laser dot will never be in focus. For imaging photographs, this is not desirable, but for detecting the LIDAR system's received pulse, amplitude is less important than timing information (i.e. pulse peak in our case). Further, this optical setup ensures that the angular extent of the dot is nearly constant over a large set of ranges. To see this, consider the second column of the table for our design. When $u < f$ and $z \gg f$, the FOV becomes $2 \operatorname{atan}\left(\frac{A(f-u)}{2uf}\right)$. Suppose $u \ll f$, then we can rewrite as $2 \operatorname{atan}\left(\frac{A(1-\frac{u}{f})}{2u}\right)$, which becomes $2 \operatorname{atan}\left(\frac{A}{2u}\right)$, which is near-constant. This is supported by simulations discussed in the main paper in Figures 2 and 3.

Of course, for the conventional approach, when $u = f$, there is a low FOV since the laser dot is sharply in focus. This is supported by simulations in Figures 2 and 3 in the main paper, for settings of $f = 15mm, A = 100mm$, over a range of sensor sizes and ranges. Therefore, the FOV degenerates to a small value, where received radiance is also the highest. Our design does not suffer this depth-dependent FOV variation and is consistent across the range. However, as shown in the right of the figure, this results in a low received radiance since the system is always defocused. In practice we find the consistent FOV to be more valuable than received radiance, and, further, depth completion can improve raw measurements.

B.1. Analysis of Sensor Design Tradeoffs

Retro-reflective receivers: If high-quality lasers such as erbium fiber lasers [41] are used, where M is near-unity, then these can be coupled with a co-located receiver and a beamsplitter, as shown in Fig. 2I(a), where the detector lens distance is equal to the focal length $u = f$. Consider the second column from Ta-

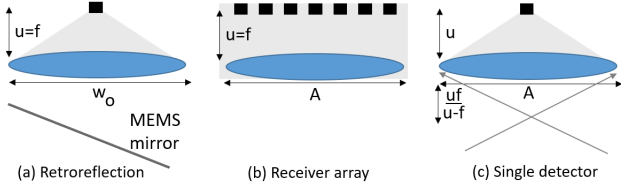


Figure A1: Ray diagrams of designs

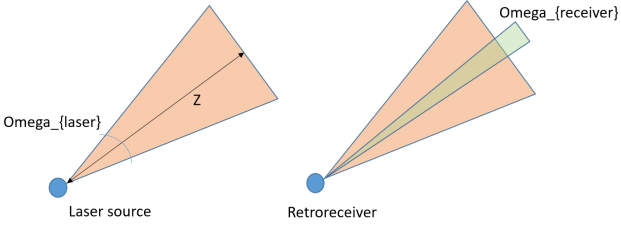


Figure A2: Retroreflective Received Radiance

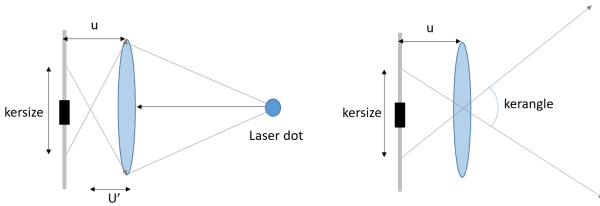


Figure A3: Single Detector Received Radiance

ble 2. The ratio of retro-reflective volume to our sensor’s volume is $\frac{w_o}{A}$, which is usually less than one, since MEMS mirrors are small.

In other words, retro-reflective designs are smaller than ours. The small retroreflective design also has the optimal FOV of the MEMS, due to co-location. Our design does have a received radiance advantage, since retroreflection requires the MEMS mirror to be the aperture for both receiver/transmitter. Fig. 3(Ia) shows how this advantage eventually trumps other factors such as laser quality ($M = 1$) or large mirrors. In the extreme case of low-cost diodes, Fig. 3(Ib), our sensor has higher received radiance at close ranges too.

Receivers arrays: If cost and size are not issues, the receiver can be made large, such as a custom-built, large SPAD array [8] or a parabolic concentrator for $1.5mm$ detectors [41]. Comparing such arrays’ volume, in Table 2’s second column, we can easily see the cuboid-cone ratio of $12/\pi$ favors our design, and is unsurprisingly shown in Fig. 3(II) (left) across multiple focal lengths.

On the other hand, it is clear that a large receiver array would have higher received radiance, due to hav-

ing a bigger effective aperture, when compared with our MEMS mirror. This is demonstrated in Fig. 3(II) (right) for the particular case of $M = 100, w_o = 5mm$, favoring our design. Despite this, large arrays have higher received radiance at all depths.

Conventional Single detector: Our approach is close to the conventional single pixel receiver, which can allow for detection over a non-degenerate FOV if it is defocused, as shown for a scanning LIDAR by [42]. When the laser dot is out of focus, some part of it activates the single photodetector. If the laser dot is in focus, the activation area available is smaller, but more concentrated. Next we describe and analyze our modification to the conventional single detector.